2014

# Coastal defence through wave farms

Abanades, J

http://hdl.handle.net/10026.1/4556

# Coastal defence through wave farms

J. Abanades[1*], D. Greaves[1], G. Iglesias[1]

[1] Plymouth University, School of Marine Science and Engineering, Marine Building, Drake Circus, Plymouth PL4 8AA, UK

The possibility of using wave farms for coastal defence warrants investigation because wave energy is poised to become a major renewable in many countries over the next decades. The fundamental question in this regard is whether a wave farm can be used to reduce beach erosion under storm conditions. If the answer to this question is positive, then a wave farm can have coastal defence as a subsidiary function, in addition to its primary role of producing carbon-free energy. The objective of this work is to address this question by comparing the response of a beach in the face of a storm in two scenarios: with and without the wave farm. For this comparison a set of *ad hoc* impact indicators is developed: the Bed Level Impact (*BLI*), beach Face Eroded Area (*FEA*), Non-dimensional Erosion Reduction (*NER*), and mean Cumulative Eroded Area (*CEA*); and their values are determined by means of two coupled models: a high-resolution wave propagation model (SWAN) and a coastal processes model (XBeach). The study is conducted through a case study: Perranporth beach (UK). Backed by a well-developed dune system, Perranporth has a bar between -5 m and -10 m. The results show that the wave farm reduces the eroded volume by as much as 50 per cent and thus contributes effectively to coastal protection. This synergy between marine renewable energy and coastal defence may well contribute to improving the viability of wave farms through savings in conventional coastal protection.

*Corresponding author; e-mail: Javier.abanadestercero@plymouth.ac.uk, tel.: +44.(0)7583544041.

## 1. INTRODUCTION

A wave farm extracts energy from the waves through Wave Energy Converters (WECs). Previous studies on the impact of wave farms on wave conditions (Beels et al., 2010; Iglesias and Carballo, 2014; Mendoza et al., 2014; Millar et al., 2007; Monk et al., 2013; Palha et al., 2010; Ruol et al., 2011; Rusu and Guedes Soares, 2013; Zanuttigh and Angelelli, 2013) demonstrated a significant reduction in the wave height in the lee of the wave farm. A sensitivity analysis of this reduction with different wave farm layouts was conducted by Carballo and Iglesias (2013). Abanades et al. (2014) studied the effects of the energy extraction by the wave farm on the beach profile (2D), analysing the evolution of several profiles during 6 months. This paper goes a step further by transcending the cross-shore (2D) analysis and examining the impact of wave energy exploitation on beach morphology (3D) – an aspect that has not been addressed so far, and whose importance can hardly be overstated in view of the intensive development of this novel renewable.

In this context, this work has a threefold objective: (i) to compare the response of a beach under storm conditions with and without a wave farm through a case study; (ii) to assess whether the nearshore attenuation of wave energy caused by the wave farm results in a reduction in the erosion on the beach; and, on these grounds, (iii) to establish whether a wave farm can contribute to coastal protection.

For the case study, a high-resolution wave propagation model coupled to a 2DH coastal processes model was applied in an area earmarked for wave energy development (Perranporth Beach, UK). First, the nearshore wave propagation model SWAN (Booij et al., 1996) was implemented on a high-resolution grid to resolve wave propagation past an array of WECs. The values of the wave transmission coefficients were obtained from

laboratory tests (Fernandez et al., 2012). Second, the coastal processes model XBEACH (Roelvink et al., 2006) was used to study the effect of the nearshore wave energy reduction on beach morphology. The suitability of XBEACH to model storm impact on beaches has been proven in recent work (Callaghan et al., 2013; McCall et al., 2010; Pender and Karunarathna, 2013; Roelvink et al., 2009; Splinter et al., 2014) . In this paper the response of the beach under storm conditions was examined in two scenarios: without (baseline) and with the wave farm. Finally, to analyse the results, a new suite of core impact indicators was developed and applied.

This article is structured as follows: in Section 2, the case study and data set are presented. In Section 3, the models and impact factors are described. In Section 4, the results are analysed and discussed. Finally, conclusions are drawn in Section 5.

## 2. CASE STUDY: PERRANPORTH BEACH

The impact of wave energy exploitation on the beach was carried out through a case study. The wave resource played a major role in the selection of the study site. A number of wave resource assessments, conducted at different scales and areas (Bernhoff et al., 2006; Defne et al., 2009; Gonçalves et al., 2014; Iglesias and Carballo, 2009; 2010a; 2010b; 2011; Pontes et al., 1998; Rusu and Guedes Soares, 2012; Stopa et al., 2011; Thorpe, 2001; Vicinanza et al., 2013b), highlighted the resource in the Atlantic façade of Europe. For the present study, Perranporth Beach (Figure 1) was selected; the nearby Wave Hub – a grid-connected offshore facility for sea tests of WECs – is testimony to the potential of this area for wave energy exploitation (Gonzalez-Santamaria et al., 2013; Reeve et al., 2011). Perranporth (Austin et al., 2010; Masselink et al., 2005) is a 4 km beach with a relatively flat intertidal area, tan $\beta = 0.015 – 0.025$,

and a medium sand size, $D_{50} = 0.27 – 0.29$ mm. The tidal range is 6.3 m (macro-tidal beach) and the tidal regime is semidiurnal.
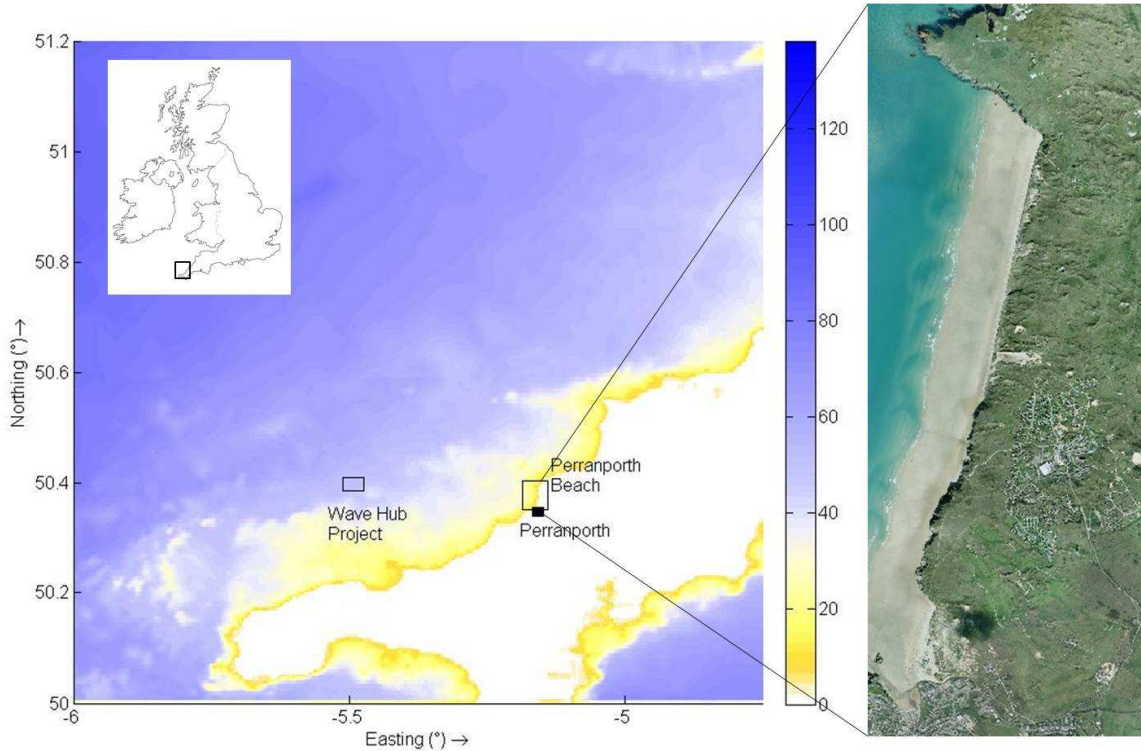


**Figure 1: Bathymetry of SW England [water depths in m] including the location of Perranporth Beach, the WaveHub Project and an aerial photo of Perranporth Beach [source: Coastal Channel Observatory].**

As regards the wave climate, Perranporth is exposed to the Atlantic swell, but also receives locally generated wind waves. The average significant wave height ($H_s$), peak period ($T_p$) and peak direction ($\theta_p$) from 2006 to 2012 (the available data) were: 1.79 m, 10.36 s and 280°, respectively. During the storm studied, from 5 December 2007 UTC 00:00 to 10 December 2007 UTC 06:00, the average wave conditions were: $H_s = 4.2$ m, $T_p = 12.1$ s and $\theta_p = 295°$.

The bathymetry of the beach was based on the data provided by the Coastal Channel Observatory. The elevation values ranged between –20 m and 25 m (Figure 2) with reference to the local chart datum (LCD). A conspicuous feature of the profile is the submarine bar between –5 m and –10 m, which will be shown to be of relevance to

4

the dynamics of the system. The bar is generally associated to the more energetic (winter) wave conditions and the consequent increase of offshore sediment transport, which results in a lowering of the intertidal beach face. Another feature of Perranporth beach is the well-developed dune system (Figure 10).
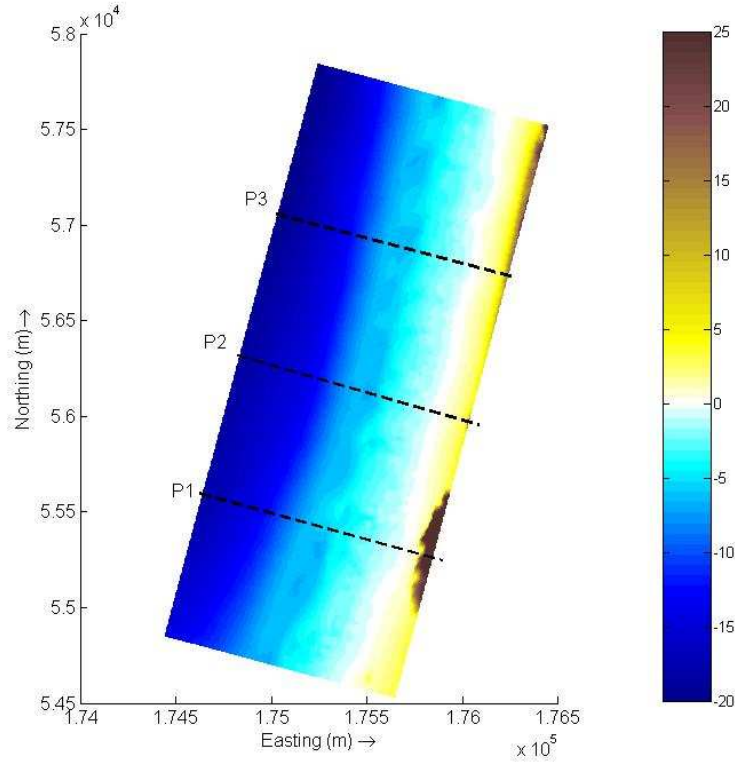


**Figure 2: Bathymetry of Perranporth Beach for the coastal processes model. Profiles P1, P2 and P3 included. Water depth in relation to local chart datum [in m].**

## 3. MATERIALS AND METHODS

### 3.1 WAVE PROPAGATION MODEL

The wave propagation was computed using SWAN v40.41 (Simulating WAves Nearshore), a third-generation spectral wave model that solves the conservation of wave action equation considering the relevant wave generation and dissipation processes,

$$\frac{\partial N}{\partial t} + \nabla \cdot \left(\vec{C}N\right) + \frac{\partial\left(C_\theta N\right)}{\partial \theta} + \frac{\partial\left(C_\sigma N\right)}{\partial \sigma} = \frac{S}{\sigma} \quad , \tag{1}$$

5

where $t$ is the time, $N$ the wave action density, $\vec{C}$ the propagation velocity in the geographical space, $\theta$ the wave direction, $\sigma$ the relative frequency, and $C_\theta$ and $C_\sigma$ the propagation velocity in the spectral space, $\theta$- and $\sigma$-space, respectively. Therefore, the first term on the left-hand side of equation (1) represents the rate of change of wave action in time, the second term describes the propagation in the geographical space, and the third and fourth terms stand for the refraction and changes in the relative frequencies respectively induced by depth and currents. On the right-hand side, $S$ is the source term representing the effects of generation, dissipation, and nonlinear wave–wave interactions.

The model was validated using data from a wave buoy at Perranporth Beach covering the period November 2007 to April 2008. The input conditions implemented in the  SWAN model were: (i) the hindcast wave data from WaveWatchIII (Tolman, 2002), a third-generation offshore wave model consisting of global and regional nested grids with a resolution of approx. 100 km; and (ii) the hindcast wind data from Global Forecast System (GFS), a global numerical weather prediction system.
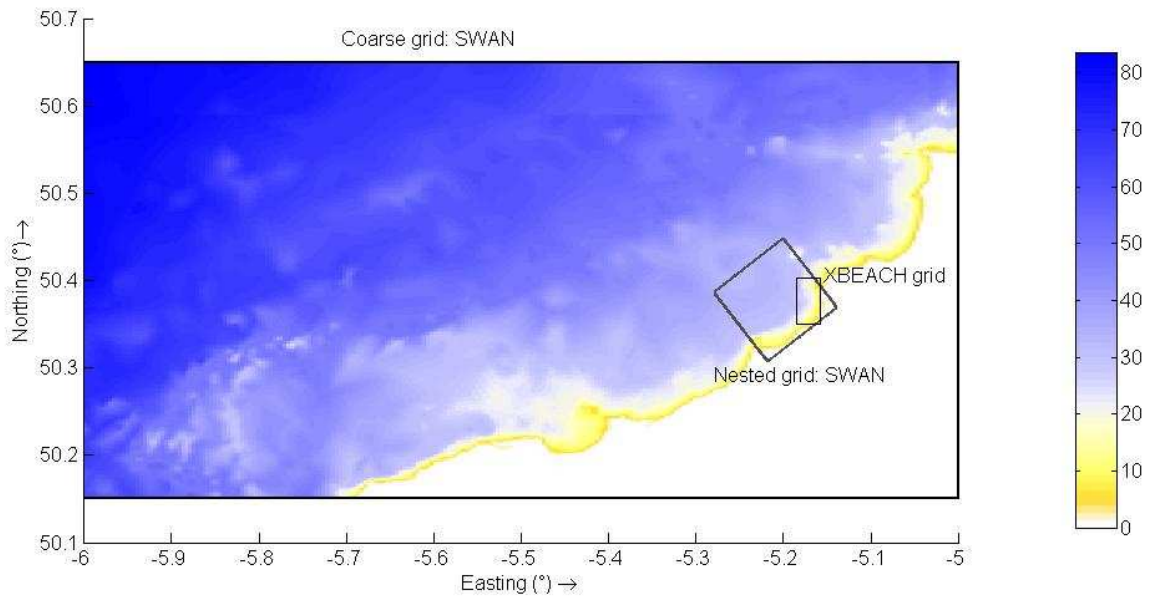


**Figure 3: Computational grids of the wave propagation and the coastal processes model [water depths in m].**

6

The computational grid consisted of two grids with different spacings (Figure 3): (i) the coarser grid extended approx. 100 km offshore and 50 km from north to south with a grid size of $400 \times 200$ m, respectively; and (ii) the finer (nested) grid covered the area of interest of approx. $15 \times 15$ km, with a resolution of $20 \times 20$ m, which allowed the exact position of the WECs to be defined within the array and the individual wake of each device to be resolved accurately. The energy transmission coefficient of the devices was input into the coastal propagation based on *ad hoc* laboratory tests (Fernandez et al., 2012). The wave farm layout consisted of 11 WaveCat WECs arranged in two rows (Figure 4), with a distance between devices of 2.2D, where $D = 90$ m is the distance between the twin bows of a single WaveCat WEC (Carballo and Iglesias, 2013).
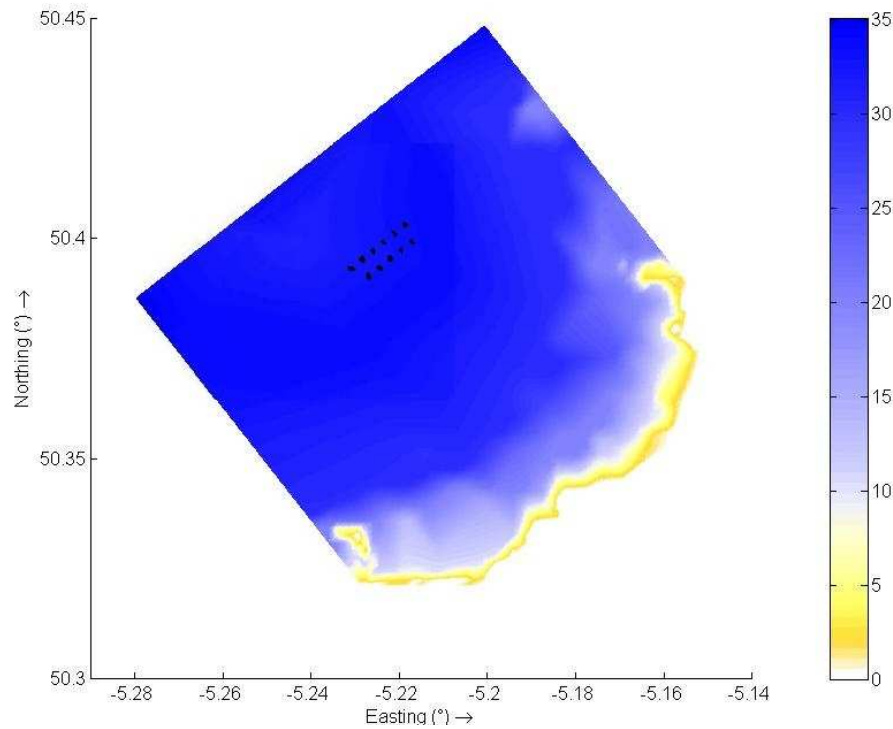


**Figure 4: Schematic of wave farm considered off Perranporth Beach, at a distance of approx. 7 km from the shoreline [water depths in m].**

7

## 3.2 COASTAL PROCESSES MODEL

Second, the coastal processes model, XBeach v1.20.3606, was coupled to the wave propagation model. XBeach is a two-dimensional model to study wave propagation, sediment transport and morphological changes of the coast. Wave processes are solved with the time-dependent wave action balance equation coupled to the roller energy equations and the nonlinear shallow water equations of mass and momentum and sediment transport is modelled with a depth-averaged advection diffusion equation (Galappatti and Vreugdenhil, 1985) on the scale of wave groups (Equation 2). The complete description of XBeach is given by Roelvink et al. (2006) or Roelvink et al. (2009).

$$\frac{\partial(hC)}{\partial t}+\frac{\partial(hCu^{E})}{\partial x}+\frac{\partial}{\partial x}\left(D_{s}h\frac{\partial C}{\partial x}\right)+\frac{\partial(hCv^{E})}{\partial y}+\frac{\partial}{\partial y}\left(D_{s}h\frac{\partial C}{\partial y}\right)=\frac{hC_{eq}-hC}{T_{S}} \qquad (2)$$

where the $x$- and $y$-coordinate represent the cross-shore and longshore direction, respectively, C is the depth-averaged sediment concentration, $D_{s}$ is the sediment diffusion coefficient, the terms $u^{E}$ and $v^{E}$ represent the Eulerian flow velocities, $T_{s}$ is the sediment concentration adaptation time scale that depends on the local water depth and the sediment fall velocity, and $C_{eq}$ is the equilibrium concentration according to the Van Rijn-Van Thiel formulation (Van Thiel de Vries, 2009), thus representing the source term in the sediment transport equation.

In the present study, the model was applied in a 2DH mode ($x, y, z$) to study the impact of the wave farm on Perranporth Beach using the results of the wave propagation model. The response of the beach during the storm period studied was investigated in both scenarios: (i) in the baseline scenario (without the wave farm), and (ii) with the wave farm, to compare the evolution of the beach and establish the contribution of a wave farm to protect the coast.

The grid covered Perranporth beach, extending 1250 m across shore and 3600 m alongshore with a resolution of 6.25 m and 18 m, respectively. The model used a number of spectral parameters obtained from the nearshore wave propagation model (the root-mean-square wave height, $H_{rms}$, mean absolute wave period, $T_{m01}$, mean wave direction, $\theta_m$, and directional spreading coefficient, $s$) as input to create time-varying wave amplitudes, i.e., the envelopes of wave groups, which have crucial importance in describing the behaviour of a beach during erosion conditions (Baldock et al., 2011).

### 3.3 IMPACT INDICATORS

The importance of monitoring and controlling coastal erosion is reflected in the number of projects delving on these matters, such as CONSCIENCE or EUROSION. In these projects, different groups of impact indicators were proposed to assess the erosion during the medium- and long-term in pilot sites. On these grounds, and taking into account the specific needs of this work, a suite of impact indicators was developed *ad hoc* to analyse the effects of the wave farm on the beach and establish the corresponding degree of coastal protection: (i) Bed Level Impact (*BLI*), (ii) each Face Eroded Area (*FEA*), (iii) Non-dimensional Erosion Reduction (*NER*), and (iv) mean Cumulative Eroded Area (*CEA*).

The bed level impact *(BLI),* with units of m in the S.I.*,* was defined as

$$BLI\left(x,y\right)=\zeta_f\left(x,y\right)-\zeta_b\left(x,y\right), \tag{3}$$

where $\zeta_f(x,y)$ and $\zeta_b(x,y)$ are the seabed level with the farm and without it (baseline), respectively, at a generic point of the beach designated by its coordinates $(x,y)$ in the horizontal reference plane. With this definition the datum for the seabed level (the elevation of the reference plane) is arbitrary, for it is the difference between the values of seabed level with and without the farm rather than their absolute values that

determine the *BLI* indicator, equation (3). Within the reference horizontal plane the *y*-coordinate axis follows the general coastline orientation, with the *y*-coordinate increasing towards the northern end of the beach. A beach profile is defined as a section of the beach with *y* = constant, and a particular point of the profile is defined by its *x*-coordinate; the orientation of the *x*-axis is taken such that *x*-values increase towards the landward end of the profile. The *BLI* indicator thus defined represents the change in bed level caused by the wave farm. A positive value signifies that the seabed level is higher with the farm than without it.

The beach face eroded area (*FEA*), with units of m$^2$ in the S.I., was defined in both scenarios, baseline (*FEA$_b$*) and with the wave farm (*FEA$_f$*):

$$FEA_b(y) = \int_{x_1}^{x_{max}} \left[ \zeta_0(x,y) - \zeta_b(x,y) \right] dx, \qquad (4)$$

$$FEA_f(y) = \int_{x_1}^{x_{max}} \left[ \zeta_0(x,y) - \zeta_f(x,y) \right] dx, \qquad (5)$$

where $\zeta_0(x,y)$ is the initial bed level at the point of coordinates $(x,y)$, and $x_1$ and $x_{max}$ are the values of the *x*-coordinate at the seaward end of the beach face and landward end of the profile, respectively. It should be noted that, unlike the bed level impact, which is a point function and therefore depends on two coordinates, $BLI = BLI(x,y)$, the beach face eroded area is a profile function, and hence depends on only one coordinate, $FEA = FEA(y)$. The *FEA* indicator can be seen as a (dimensional) parameter measuring the impact of the farm on the beach face.

The non-dimensional erosion reduction (*NER*) is also a profile function, in this case non-dimensional, defined as

$$NER(y) = 1 - (x_{\max} - x_1)^{-1} \int_{x_1}^{x_{\max}} \left[ \zeta_0(x,y) - \zeta_f(x,y) \right] \left[ \zeta_0(x,y) - \zeta_b(x,y) \right]^{-1} dx. \qquad (6)$$

It expresses the variation in the eroded area of a generic profile ($y$) brought about by the wave farm as a fraction of the total eroded area of the same profile. A positive or negative value implies a reduction or increase in the eroded area as a result of the wave farm.

Finally, the mean cumulative eroded area ($CEA$), with units of $m^2$ (or $m^3$ per linear metre of beach), was determined both in the baseline scenario ($CEA_b$) and with the wave farm ($CEA_f$). For its definition three reference profiles were considered: P1, P2 and P3 (Figure 2). For each of these the beach was divided into two parts, to the north ($CEA_b^N$ and $CEA_f^N$) and south ($CEA_b^S$ and $CEA_f^S$) of the reference profile, and the corresponding indicators were computed from

$$CEA_b^S(x) = (y_P - y_0)^{-1} \int_{y_0}^{y_P} \int_{x_0}^{x} [\zeta_0(\chi, y) - \zeta_b(\chi, y)] d\chi\, dy, \qquad (7)$$

$$CEA_f^S(x) = (y_P - y_0)^{-1} \int_{y_0}^{y_P} \int_{x_0}^{x} \left[ \zeta_0(\chi, y) - \zeta_f(\chi, y) \right] d\chi\, dy \qquad (8)$$

$$CEA_b^N(x) = (y_{\max} - y_P)^{-1} \int_{y_P}^{y_{\max}} \int_{x_0}^{x} [\zeta_0(\chi, y) - \zeta_b(\chi, y)] d\chi\, dy, \qquad (9)$$

$$CEA_f^N(x) = (y_{\max} - y_P)^{-1} \int_{y_P}^{y_{\max}} \int_{x_0}^{x} \left[ \zeta_0(\chi, y) - \zeta_f(\chi, y) \right] d\chi\, dy, \qquad (10)$$

where the variable of integration $\chi$ represents the coordinate along the profile, and $x$ and $x_0$, and $y_0$, $y_{max}$ and $y_P$ are the limits of integration along the profile and along the coast, respectively. $x_0$ is the value of the $x$-coordinate corresponding to the first point of

the profile and $x$ takes values from $x_0$ to $x_{max}$. Along the beach, $y_0$ is the value of the $y$-coordinate corresponding to the southernmost point of the beach, $y_{max}$ the northernmost point of the beach and $y_P$ the value corresponding to the reference profile. The factor represents the average cumulative eroded area of the two sections of the beach along the profile ($x$). A positive value signifies that the mean volume of material along the section of the beach is reduced compared with the initial situation (erosion).

## 4. RESULTS AND DISCUSSION

The validation of the high-resolution wave propagation model was carried out using the significant wave height ($H_s$) values from the wave buoy at Perranporth beach from November 2007 to April 2008(Abanades et al., 2014). Figure 5 shows the good fit achieved by the model. The error statistics studied for the validation confirmed that the correlation between the series achieves a Root Mean Square Error (*RMSE)* of *0.46* m and a coefficient of determination *($R^2$)* of *0.84*.
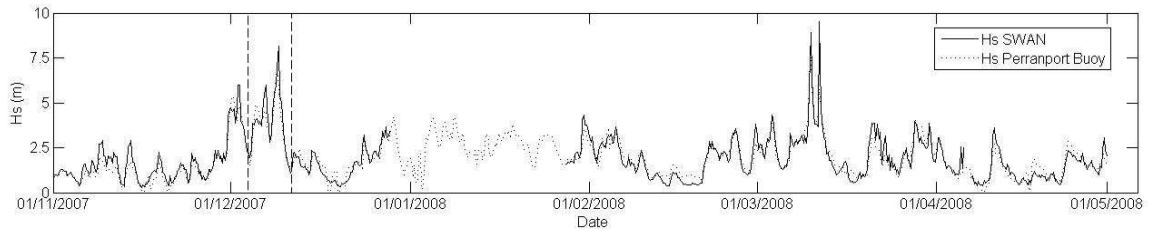


**Figure 5: Time series of simulated ($H_s$SWAN) and measured ($H_s$buoy) significant wave height to validate the high resolution wave propagation model. The storm conditions studied (from 5 Dec 2007, 00:00 UTC; to 10 Dec 2007, 18:00 UTC) to assess the impact of the wave farm are highlighted.**

The results of the wave propagation model were studied in both scenarios: baseline and in the presence of the wave farm, to observe the impact of the wave farm on the wave conditions. The reduction of the significant wave height in the lee of the farm is shown in Figure 6, in which the shadow zone downstream of each WEC is apparent.
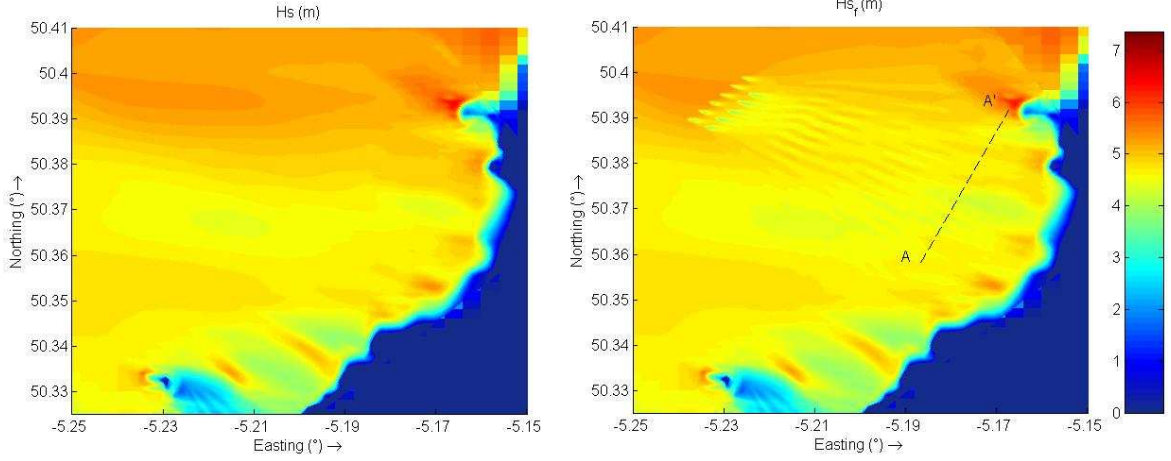
**Figure 6: Significant wave height in the baseline scenario ($H_s$) and with the wave farm ($H_{sf}$) at the first peak of the storm studied (5 Dec 2007, 18:00 UTC). [Deep water wave conditions: $H_{s0}$ = 6.89 m, $T_p$ = 15.64 s, $\theta_p$ = 268.45 °]. The line AA' is shown.**

Using this data, Figure 7 shows the reduction of the significant wave height between the scenario in the presence of the farm and the baseline scenario. The reduction within the wave farm was greater than 30%, although advancing towards the coastline from the wave farm, the difference decreased due to the wave energy being diffracted from the edges into the shadow of the farm. However, this energy was not enough to mitigate the effect of the wave farm nearshore; indeed the reduction was greater than 10 % along the 20 m contour in the northern area of the grid, which was the area most sheltered by the wave farm.
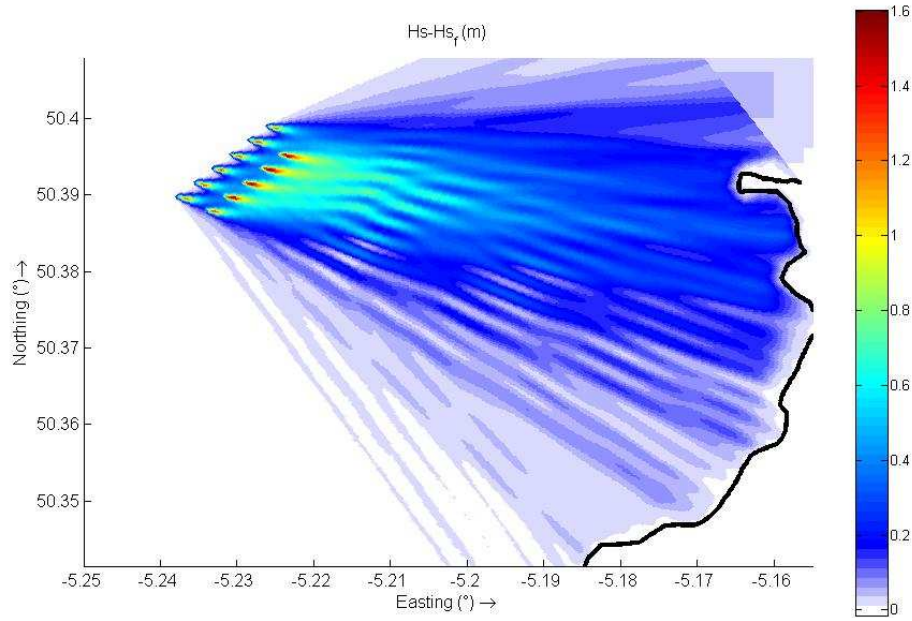
13

**Figure 7: Significant wave height difference between the baseline scenario ($H_s$) and with the wave farm ($H_{sf}$) at the first peak of the storm studied (5 Dec 2007, 18:00 UTC). The black line represents the shoreline [Deep water wave conditions: $H_{s0}$ = 6.89 m, $T_p$ = 15.64 s, $\theta_p$ = 268.45 °].**

Having investigated the effects of the wave farm on the wave conditions in its lee, the results along the line AA' (Figure 6), in approximately 20 m of water depth, were input to the coastal processes model. The significant wave height ($H_s$) across AA' in both scenarios is shown in Figure 8, where the shadow due to the wave energy absorption of each device can be readily observed. The impact of the wave farm was found to be more significant in the northern and middle areas of the beach.

The coastal processes model used the output of the wave propagation model to study how modification of the wave conditions affected the coastal processes and, consequently, the beach morphology during the period studied. The longshore and offshore/onshore sediment transport was studied through a suite of core impact indicators, defined in Section 3.2, to assess the impact of the wave farm.
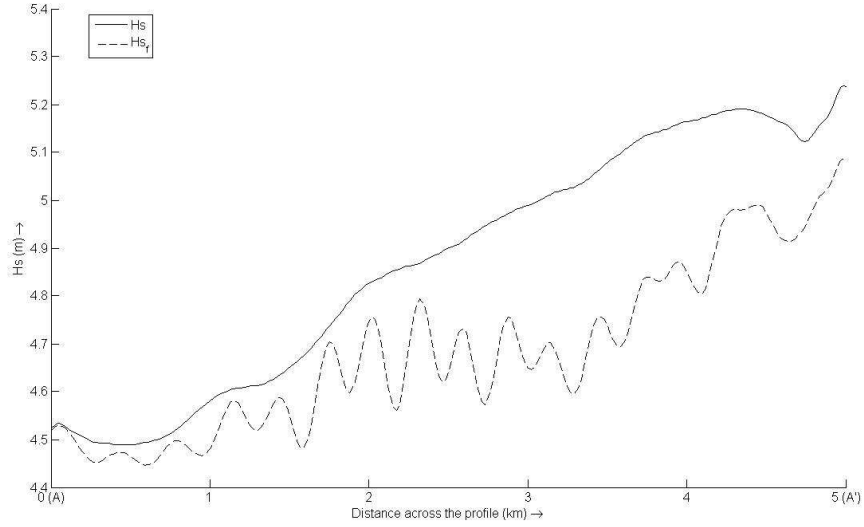
14

**Figure 8: Significant wave height in the baseline scenario ($H_s$) and in the presence of the farm ($H_{sf}$) across the line AA' at the first peak of the storm studied (5 Dec 2007, 18:00 UTC). [Deep water wave conditions: $H_{s0}$ = 6.89 m, $T_p$ = 15.64 s, $\theta_p$ = 268.45 °].**

The sea bed level was studied at the end of the time period studied in both scenarios: in the presence of the farm and in the baseline scenario, through the BLI factor (Figure 9). The reduction of the erosion was observed mainly in the dune in the back of the beach, reaching values greater than 4 m, a result of the wave energy extraction by the wave farm. A reduction of the erosion was also found along the bar in water depth between 5 and 10 m, especially in the middle area of the beach where the *BLI* parameter reached values of 0.5 m. On the other hand, the material eroded from the dune was moved to the lower section of the profile, between the bar and the dune, which resulted in the *BLI* parameter taking negative values in the region of –0.5 m.
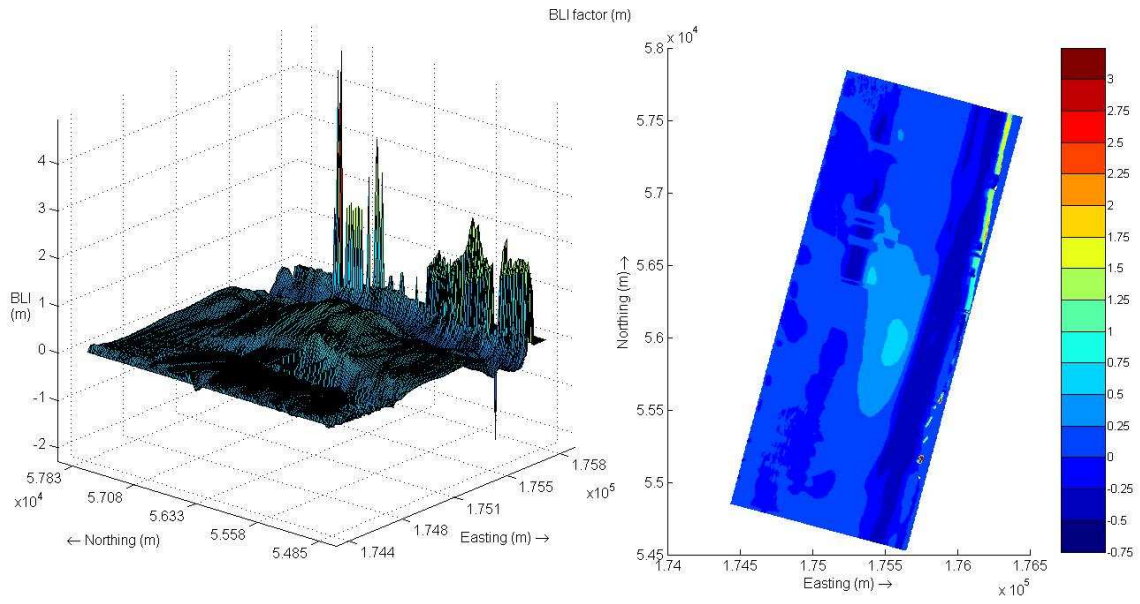
**Figure 9: Bed level impact (*BLI*) at the end of the time period studied [10 Dec 2007, 06:00 UTC].**

On this basis, the impact of the wave farm on the bed level is shown in Figure 10 along three profiles: P1 (south), P2 (middle) and P3 (north), shown in Figure 2. The initial profile ($\zeta_0$) was compared with the profiles at the end of the storm studied in both scenarios: the baseline scenario ($\zeta_b$) and in the presence of the farm ($\zeta_f$). The results show a more significant effect on profiles P3 and P2, in the northern and middle areas of the beach, than on P1, in accordance with the wave conditions shown in Figure 8. As may be observed in Figure 9, the effects of the wave farm are more pronounced in the intertidal area over the mean water level (at the landward end of the profiles) and over the bar. Furthermore, Profile P3 shows that the wave farm not only reduced the eroded area but also altered the sediment transport pattern, moving the initial erosion point up to 30 m towards the shoreline.
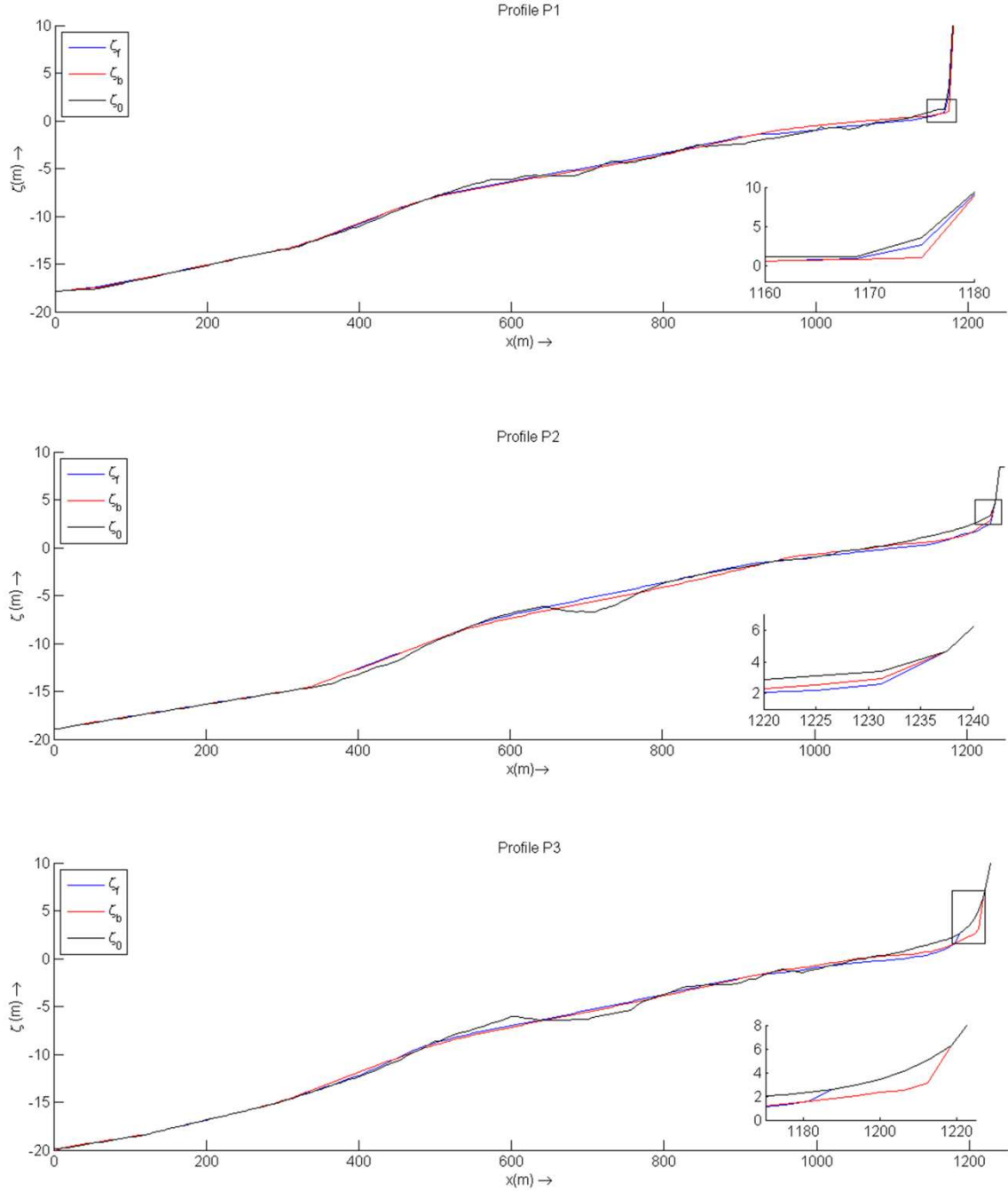
16

**Figure 10: Bed level at Profiles P1, P2 and P3: initial ($\zeta_0$) [05 Dec 2007, 00:00 UTC] and at the end of the simulation in the baseline scenario ($\zeta_b$) and with the wave farm ($\zeta_f$) [10 Dec 2007, 06:00 UTC].**

The volume of material moved per linear metre along the beach ($y$) was studied through the mean Cumulative Eroded Area (*CEA*). This indicator showed the difference in material eroded along the profile ($x$) between the initial and final points of the time period studied in both scenarios: baseline (*CEA$_b$*) and with the wave farm (*CEA$_f$*).

17

Figure 11 shows the results in the southern and northern areas across the different reference profiles P1 (south), P2 (middle) and P3 (north). In the case of profile P2, the wave farm modified the sediment transport patterns significantly: whereas erosion was reduced in the northern area of the beach, in the southern area the material eroded increased for water depths below 5 m. As for profile P1, the northern area of the beach presented less sediment transport in the presence of the wave farm for water depths over 7 m, while accretion occurred for water depths below 7 m. In the case of profile P3, the sediment transport patterns were hardly affected by the wave farm for water depths over 5 m, but in water depths below 5 m erosion decreased in the southern area of the beach. In summary, in the baseline scenario (without the wave farm) accretion was found to occur in the deeper sections of the profile in the northern area owing to the offshore sediment transport from the beach face and the submarine bar. In the presence of the wave farm, however, the erosion of the beach face and submarine bar was significantly reduced. As a result of this, and of the increase of the southward sediment transport, the accretion of the deeper sections of the profile in the northern area that occurred in the baseline scenario was replaced by accretion in the southern area of the beach for values of the $x$ coordinate greater than 600 m (as may be seen on profiles P2 and P3).
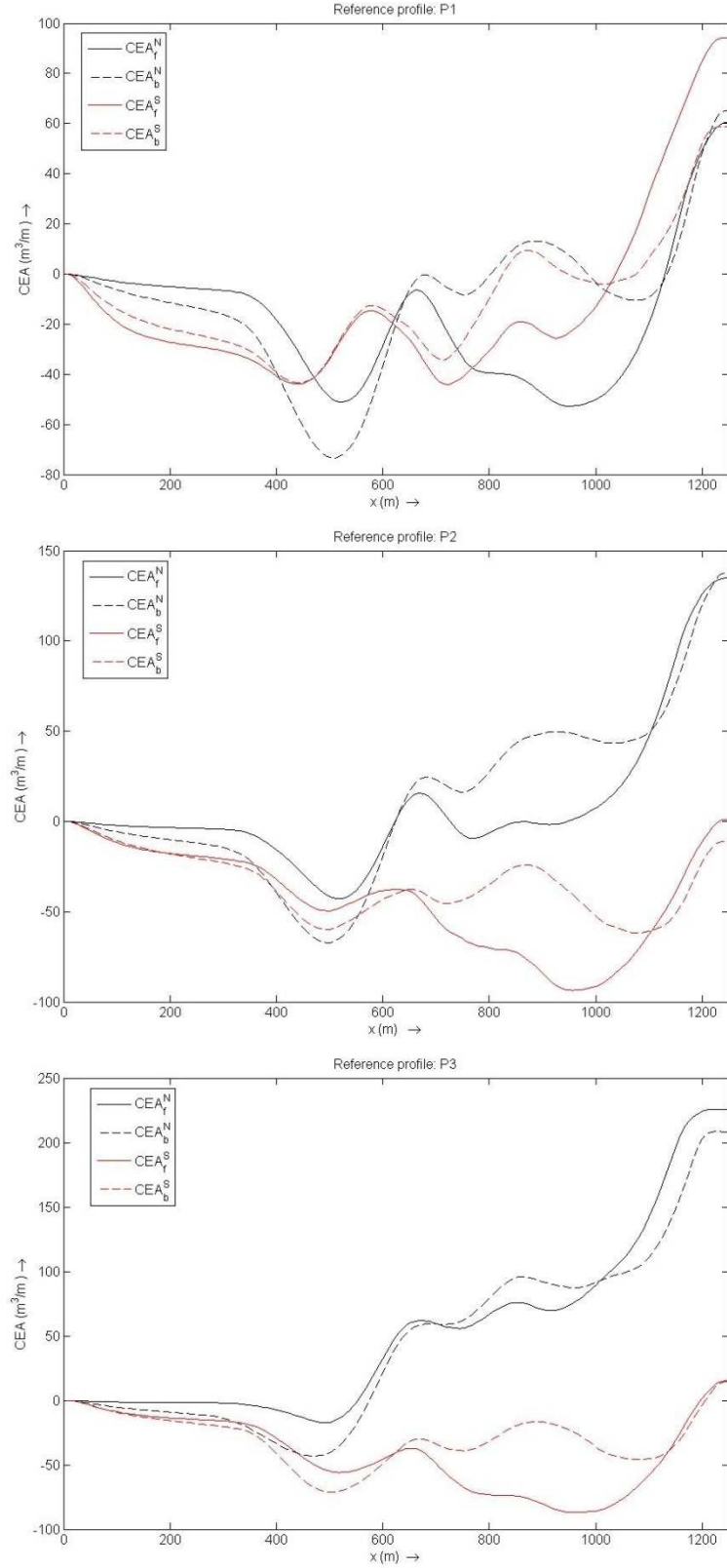
**Figure 11: Mean cumulative eroded area in the baseline scenario ($CEA_b$) and in presence of the wave farm ($CEA_f$) in the southern area (in red) and northern area (in black) across each of the reference profiles P1, P2 and P3, at the end of the time period studied [10 Dec 2007, 06:00 UTC]. The x-coordinate represents the distance along the profile, with $x = 0$ the most offshore point.**

Finally, the results of the beach face eroded area (*FEA*) confirmed the contribution of the wave farm to reducing erosion. Figure 12 shows the evolution of the erosion along Perranporth Beach ($y = 0$ corresponds to the southernmost point of the beach). The most severe erosion took place in the southernmost area of the beach, which is not backed by the dune system, and the northern area, where the waves were higher (Figure 8). As regards the efficacy of the wave farm for coastal protection, the reduction in erosion was more significant in the northern area of the beach than in the south and in the middle. In Figure 13, the non-dimensional erosion reduction (*NER*) is represented on the basis of the results of the eroded area in the beach face, confirming that the wave farm attenuated the erosion in the north of the beach, with values over 50%. As regards the southern area of the beach, 500 m $< y <$ 1500 m, the *NER* factor fluctuated strongly, due to isolated responses of different points of the profiles.
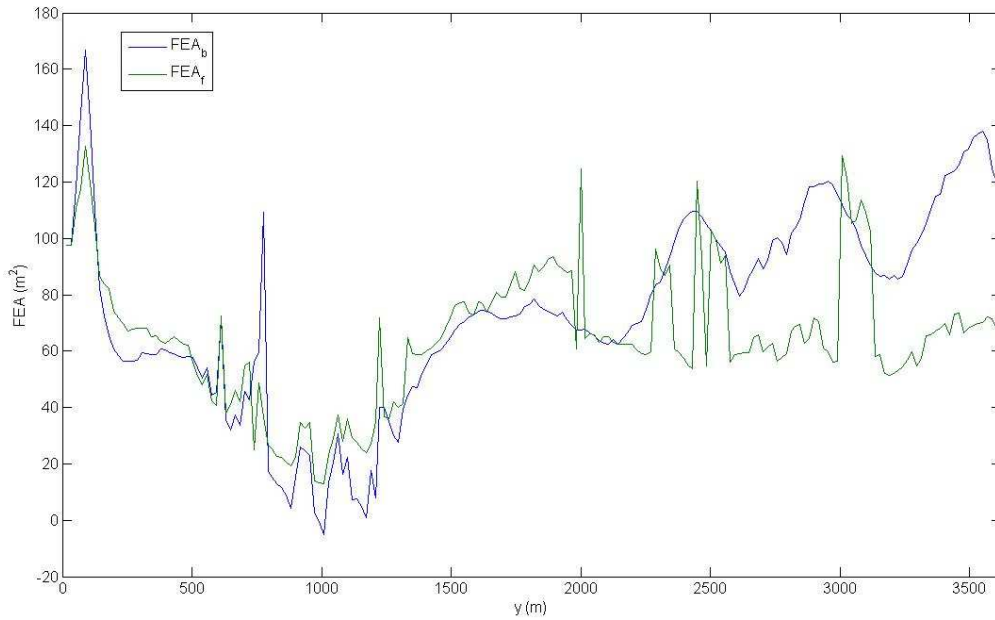


**Figure 12: Beach face eroded area in two scenarios: baseline (*FEA_b*) and with the wave farm (*FEA_f*) along Perranporth Beach (*y* - coordinate, with *y* increasing towards the north of the beach) at the end of the time period studied [10 Dec 2007, 06:00 UTC].**
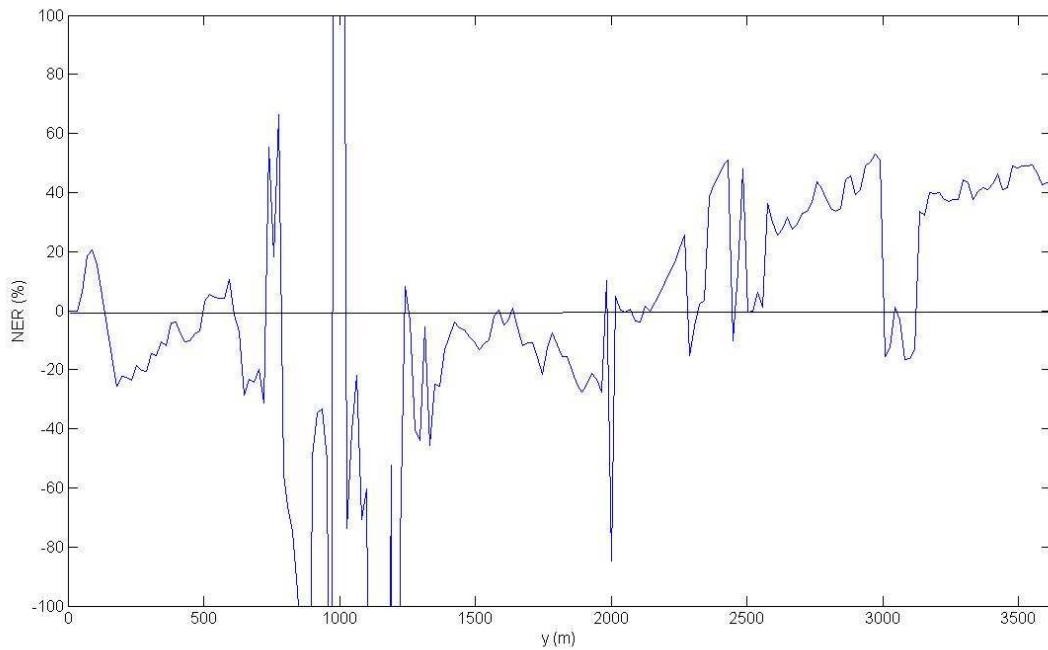
**Figure 13: Non-dimensional erosion reduction (*NER*) at the beach face along Perranporth Beach (*y* - coordinate, with *y* increasing towards the north of the beach) at the end of the time period studied [10 Dec 2007, 06:00 UTC].**

The results obtained in this work seem to lend credence to the hypothesis formulated at the outset, namely that a wave farm can serve as a coastal defence measure. It is important to bear in mind, however, that these results, and in particular its quantitative aspects, were derived for a specific case study: a beach with a bar between -5 m and -10 m backed by a well-developed dune system and under the attack of a storm of certain characteristics. Needless to say, these quantitative results may not apply to other situations. Furthermore, the study constitutes a first approximation to the potential of wave farms for coastal defence, a complex question owing to the many processes involved. On open oceanic coasts, such as the present case study, most sediment transport takes place in the surf zone, with wave-induced currents playing the main role. It is well known that on these coasts the fundamental effect of the tide as regards sediment dynamics is a direct result of the variation of the water level, namely the extension of the section of the beach profile on which the energy of the breaking waves

21

is dissipated. This fundamental effect of the tide was taken into account in this work by including the tide in the morphodynamic model. As regards the interaction between the waves and tidal currents in the area, highlighted in a recent work by Gonzalez-Santamaria et al. (2013), the authors look forward to continuing this line of work in the near future by considering the effects that such interaction could have on wave propagation and, consequently, on the sediment transport patterns at Perranporth. So far this interaction has not been considered, and could be a source of uncertainty in the results. Other sources of uncertainty could be the limitations of the 2DH modelling approach and the operational procedures of the wave farm under storm conditions, which are not easy to establish at this point, when no wave farm is operational yet. As indicated, the investigation of the applicability of wave farms to coastal defence is far from finished, and these uncertainties will hopefully be tackled as wave energy progresses to become a fully-fledged renewable energy source.

## 5. CONCLUSIONS

This paper dealt with the impact of a wave farm on a sandy coast through a case study. A coastal wave model was coupled to a coastal processes model to investigate how the attenuation of wave energy caused by the wave farm affects the morphology of a beach in its lee. The wave propagation model was used to study the interaction of the wave farm with the wave field. It was implemented on a high-resolution computational grid, which enabled to resolve the wakes of the individual WECs forming the farm. Energy extraction by the WECs led to a reduction of the significant wave height, which exceeded 30% of the incident significant wave height immediately in the lee of the farm, decreased towards the shoreline; in a water depth of 20 m this reduction was approximately 10%. The impact of the farm on the nearshore wave conditions was

found to be more significant in the northern area of the beach owing to the incoming wave direction and local bathymetry. Based on the results of the wave propagation model, the coastal processes model was applied to assess the response of the beach under storm conditions in two scenarios: without the wave farm (baseline) and with it. By comparing both scenarios the effects of the wave farm on the beach morphology were established.

For this purpose a new suite of core impact indicators was developed: the bed level impact (*BLI*), beach face eroded area (*FEA*), non-dimensional erosion reduction (*NER*) and cumulative eroded area (*CEA*). The bed level impact (*BLI*) evidenced the capacity of the wave farm to significantly reduce erosion in two sections of the beach profile: (i) over the submarine bar, where the seabed drop caused by erosion was reduced by more than 0.5 m (*BLI* greater than 0.5 m); and (ii) at the beach face, where the *BLI* exceeded 4 m at different positions along the beach. The variation along the 3.6 km long beach in the area eroded from the beach face was assessed by means of the *FEA* and *NER* indicators. The wave farm was found to result in a non-dimensional erosion reduction above 50% along a 1.5 km stretch in the north section of the beach. This pronounced impact of wave energy extraction was confirmed with the *CEA* indicator.

For each of the reference profiles P1, P2 and P3, the north and south sections experience different behaviour. In the north sections, in the absence of the farm accretion occurred in the deeper section of the profile at the expense of erosion over the bar and intertidal areas; in contrast, no accretion in the deeper section was observed in the presence of the wave farm – in line with the aforementioned reduction in the erosion over the bar and beach face. In the south sections, while there are small differences in the deeper parts of the profile, in the upper parts (intertidal areas) an increase of the accretion was found with the wave farm. This would appear to indicate that, whereas in

the baseline scenario substantial offshore sediment transport occurs, in particular in the north sections, leading to accretion in the deeper section of the profile at the expense of the material eroded from the beach face and the bar, the wave farm modifies this pattern by reducing the offshore sediment transport and increasing the southbound longshore sediment transport, resulting in accretion throughout the profile in the southern part of the beach.

To sum up, the nearshore wave farm was found to cause a substantial impact on the beach dynamics. Erosion, especially at the beach face, was significantly reduced, which lends credence to the hypothesis that a wave farm can serve as a coastal defence measure. This synergy between coastal protection and energy production enhances the economic viability of wave energy. Furthermore, the application of wave farms to coastal protection has an advantage from the standpoint of coastal management, at least if floating wave energy converters are considered (as in this work) – the effectiveness of the wave farm as a coastal defence mechanism is not affected by sea level change.

## 6. REFERENCES

Abanades, J., Greaves, D. and Iglesias, G., 2014. Wave farm impact on the beach profile: A case study. Coastal Engineering, 86(0): 36-44.

Austin, M. et al., 2010. Temporal observations of rip current circulation on a macro-tidal beach. Continental Shelf Research, 30(9): 1149-1165.

Baldock, T.E. et al., 2011. Large-scale experiments on beach profile evolution and surf and swash zone sediment transport induced by long waves, wave groups and random waves. Coastal Engineering, 58(2): 214-227.

Baldock, T.E., Manoonvoravong, P. and Pham, K.S., 2010. Sediment transport and beach morphodynamics induced by free long waves, bound long waves and wave groups. Coastal Engineering, 57(10): 898-916.

Beels, C., Troch, P., De Visch, K., Kofoed, J.P. and De Backer, G., 2010. Application of the time-dependent mild-slope equations for the simulation of wake effects in the lee of a farm of wave dragon wave energy converters. Renewable Energy, 35(8): 1644-1661.

Bernhoff, H., Sjöstedt, E. and Leijon, M., 2006. Wave energy resources in sheltered sea areas: A case study of the baltic sea. Renewable Energy, 31(13): 2164-2170.

Booij, N., Holthuijsen, L. and Ris, R., 1996. The" swan" wave model for shallow water. Coastal engineering conference, p.^pp. 668-676.

Booij, N., Ris, R.C. and Holthuijsen, L.H., 1999. A third-generation wave model for coastal regions: 1. Model description and validation. Journal of Geophysical Research: Oceans, 104(C4): 7649-7666.

Callaghan, D.P., Ranasinghe, R. and Roelvink, D., 2013. Probabilistic estimation of storm erosion using analytical, semi-empirical, and process based storm erosion models. Coastal Engineering, 82(0): 64-75.

Carballo, R. and Iglesias, G., 2013. Wave farm impact based on realistic wave-wec interaction. Energy, 51: 216-229.

Clément, A. et al., 2002. Wave energy in europe: Current status and perspectives. Renewable and Sustainable Energy Reviews, 6(5): 405-431.

Cornett, A.M., 2008. A global wave energy resource assessment. ISOPE--579

Cowell, P. and Thom, B., 1994. Morphodynamics of coastal evolution. Cambridge University Press, Cambridge, United Kingdom and New York, NY, USA.

Defne, Z., Haas, K.A. and Fritz, H.M., 2009. Wave power potential along the atlantic coast of the southeastern USA. Renewable Energy, 34(10): 2197-2205.

Egbert, G.D., Bennett, A.F. and Foreman, M.G., 1994. Topex/poseidon tides estimated using a global inverse model. Journal of Geophysical Research: Oceans (1978–2012), 99(C12): 24821-24852.

European Commission, 2007. A european strategic energy technology plan (set-plan)–towards a low-carbon future, Communication from the Commission to the Council, the European Parliament, the European Economic and Social Committee and the Committee of the Regions, COM (2007).

Falcão, A.F.O., 2007. Modelling and control of oscillating-body wave energy converters with hydraulic power take-off and gas accumulator. Ocean Engineering, 34(14–15): 2021-2032.

Falcão, A.F.O. and Justino, P.A.P., 1999. Owc wave energy devices with air flow control. Ocean Engineering, 26(12): 1275-1295.

Fernandez, H. et al., 2012. The new wave energy converter wavecat: Concept and laboratory tests. Marine Structures, 29(1): 58-70.

Galappatti, G. and Vreugdenhil, C., 1985. A depth-integrated model for suspended sediment transport. Journal of Hydraulic Research, 23(4): 359-377.

Gonçalves, M., Martinho, P. and Guedes Soares, C., 2014. Wave energy conditions in the western french coast. Renewable Energy, 62(0): 155-163.

Gonzalez-Santamaria, R., Zou, Q.-P. and Pan, S., 2013. Impacts of a wave farm on waves, currents and coastal morphology in south west england. Estuaries and Coasts: 1-14.

Gonzalez, R., Zou, Q. and Pan, S., 2012. Modelling of the impact of a wave farm on nearshore sediment transport. Proceedings of the international conference of Coastal Engineering 2012.

Iglesias, G. and Carballo, R., 2009. Wave energy potential along the death coast (spain). Energy, 34(11): 1963-1975.

Iglesias, G. and Carballo, R., 2010a. Offshore and inshore wave energy assessment: Asturias (n spain). Energy, 35(5): 1964-1972.

Iglesias, G. and Carballo, R., 2010b. Wave energy and nearshore hot spots: The case of the se bay of biscay. Renewable Energy, 35(11): 2490-2500.

Iglesias, G. and Carballo, R., 2011. Choosing the site for the first wave farm in a region: A case study in the galician southwest (spain). Energy, 36(9): 5525-5531.

Iglesias, G. and Carballo, R., 2014. Wave farm impact: The role of farm-to-coast distance. Renewable Energy (in press).

Iglesias, G., Carballo, R., Castro, A. and Fraga, B., 2008. Development and design of the wavecat™ energy converter. Coastal Engineering: 3970-3982.

Jamal, M.H., Simmonds, D.J., Magar, V. and Pan, S., 2011. Modelling infiltration on gravel beaches with an xbeach variant. Proceedings of the International Conference on Coastal Engineering, 1(32): sediment. 41.

Kofoed, J.P., Frigaard, P., Friis-Madsen, E. and Sørensen, H.C., 2006. Prototype testing of the wave energy converter wave dragon. Renewable Energy, 31(2): 181-189.

Masselink, G., Evans, D., Hughes, M.G. and Russell, P., 2005. Suspended sediment transport in the swash zone of a dissipative beach. Marine Geology, 216(3): 169-189.

McCall, R.T. et al., 2010. Two-dimensional time dependent hurricane overwash and erosion modeling at santa rosa island. Coastal Engineering, 57(7): 668-683.

Mendoza, E. et al., 2014. Beach response to wave energy converter farms acting as coastal defence. Coastal Engineering, 87(0): 97-111.

Millar, D.L., Smith, H.C.M. and Reeve, D.E., 2007. Modelling analysis of the sensitivity of shoreline change to a wave farm. Ocean Engineering, 34(5-6): 884-901.

Monk, K., Zou, Q. and Conley, D., 2013. An approximate solution for the wave energy shadow in the lee of an array of overtopping type wave energy converters. Coastal Engineering, 73: 115-132.

Nørgaard, J.H., Andersen, T.L. and Kofoed, J.P., 2011. Wave dragon wave energy converters used as coastal protection, Proceedings of the international conference of Coastal Structures 2011. Imperial College Press., Yokohama.

Palha, A., Mendes, L., Fortes, C.J., Brito-Melo, A. and Sarmento, A., 2010. The impact of wave energy farms in the shoreline wave climate: Portuguese pilot zone case study using pelamis energy wave devices. Renewable Energy, 35(1): 62-77.

Pender, D. and Karunarathna, H., 2012. Modeling beach profile evolution – a statistical–process based approach. 2012.

Pender, D. and Karunarathna, H., 2013. A statistical-process based approach for modelling beach profile variability. Coastal Engineering, 81(0): 19-29.

Pontes, M. et al., 1998. The european wave energy resource. 3rd European Wave Energy Conference, Patras, Greece, p.^pp.

Pontes, M. et al., 1996. Weratlas–atlas of wave energy resource in europe. Report to the European Commission, JOULE II Programme, 96p.

Reeve, D.E. et al., 2011. An investigation of the impacts of climate change on wave energy generation: The wave hub, cornwall, uk. Renewable Energy, 36(9): 2404-2413.

Roelvink, D. et al., 2009. Modelling storm impacts on beaches, dunes and barrier islands. Coastal Engineering, 56(11–12): 1133-1152.

Roelvink, J. et al., 2006. Xbeach model description and manual. UNESCO-IHE Institute for Water Education.

Ruol, P., Zanuttigh, B., Martinelli, L., Kofoed, P. and Frigaard, P., 2011. Near-shore floating wave energy converters: Applications for coastal protection, Proceedings of the international conference of Coastal Engineering 2010, Shanghai.

Rusu, E. and Guedes Soares, C., 2013. Coastal impact induced by a pelamis wave farm operating in the portuguese nearshore. Renewable Energy, 58(0): 34-49.

Rusu, L. and Guedes Soares, C., 2012. Wave energy assessments in the azores islands. Renewable Energy, 45(0): 183-196.

Scott, T., Masselink, G. and Russell, P., 2011. Morphodynamic characteristics and classification of beaches in england and wales. Marine Geology, 286(1–4): 1-20.

Splinter, K.D., Carley, J.T., Golshani, A. and Tomlinson, R., 2014. A relationship to describe the cumulative impact of storm clusters on beach erosion. Coastal Engineering, 83(0): 49-55.

Stopa, J.E., Cheung, K.F. and Chen, Y.-L., 2011. Assessment of wave energy resources in hawaii. Renewable Energy, 36(2): 554-567.

Thorpe, T., 2001. The wave energy programme in the uk and the european wave energy network.

Tolman, H.L., 2002. User manual and system documentation of wavewatch-iii version 2.22.

Van Dongeren, A.R., Battjes, J. and Svendsen, I., 2003. Numerical modeling of infragravity wave response during delilah. Journal of Geophysical Research, 108(C9): 3288.

Van Thiel de Vries, J., 2009. Dune erosion during storm surges. PhD Thesis Thesis, Delft University of Technology.

Vicinanza, D., Contestabile, P. and Ferrante, V., 2013a. Wave energy potential in the north-west of sardinia (italy). Renewable Energy, 50: 506-521.

Vicinanza, D., Contestabile, P. and Ferrante, V., 2013b. Wave energy potential in the north-west of sardinia (italy). Renewable Energy, 50(0): 506-521.

Vidal, C., Méndez Fernando, J., Díaz, G. and Legaz, R., 2007. Impact of santoña wec installation on the littoral processes. Proceedings of the 7th European wave and tidal energy conference, Porto, Portugal.

Williams, J.J., de Alegría-Arzaburu, A.R., McCall, R.T. and Van Dongeren, A., 2012. Modelling gravel barrier profile response to combined waves and tides using xbeach: Laboratory and field results. Coastal Engineering, 63(0): 62-80.

Zanuttigh, B. and Angelelli, E., 2013. Experimental investigation of floating wave energy converters for coastal protection purpose. Coastal Engineering, 80: 148-159.